IEEE TRANSACTIONS ON MAGNETICS, VOL. 38, NO. 2, MARCH 2002

Eddy Current Calculations in Three-Dimensional Moving Structures

Francesca Rapetti, Yvon Maday, Frédéric Bouillault, and Adel Razek, *Fellow, IEEE*

***Abstract*—A nonconforming nonoverlapping domain decomposition method to approximate the eddy current problem, formulated in terms of the modified magnetic vector potential, in three-dimensional (3-D) moving structures, is presented. This approximation allows for nonmatching grids at the sliding interface and is based on the mortar element method combined with edge elements in space and finite differences in time. Numerical results illustrate how the method works and the influence of eddy currents on the field distribution.**

***Index Terms*—Please provide indexing terms. Send a blank e-mail to keywords@ieee.org for a list of suggested keywords.**

I. Introduction

THIS contribution deals with the numerical simulation of eddy currents in three-dimensional (3-D) moving rigid bodies. Such a problem arises, for example, from the modeling of electromechanical systems. We address the question of how to calculate the electromagnetic fields if the motion of the bodies is known in advance. In the presence of moving structures, we can work in Euler variables, adding a convective term in the equations or in Lagrange ones. The second choice may be, physically and computationally, more convenient if we use a method that allows to use nonmatching grids at the sliding interface. The problem of dealing with nonmatching grids has been faced for a long time (see [6] for a short overview on the subject) and the existing methods are difficult to be applied for 3-D modeling. The *mortar element method* (see [2] for its mathematical analysis in the Maxwell's equations framework and [4] for its first application to magnetostatics in 3-D) is a nonconforming nonoverlapping domain decomposition technique which allows for independent meshes in adjacent subdomains. The idea of the method is to weakly impose the transmission conditions at the interfaces by means of Lagrange multipliers suitably chosen to ensure optimal properties on the discrete problem. The numerical results we present here correspond to the first application of the proposed method to magnetodynamics. They constitute an encouraging step toward more realistic applications.

Manuscript received July 5, 2001; revised October 25, 2001.

F. Rapetti is with the Lab. J.A.Dieudonne UMR 6621 CNRS, University of Nice–Sophia Antipolis, 06108 Nice Cedex 2, France (e-mail: frapetti@unice.fr).

Y. Maday is with the Lab. d'Analyse Numérique, UMR 7598 CNRS, University of Paris 6, 75252 Paris, France (e-mail: maday@ann.jussieu.fr).

F. Bouillault and A. Razek are with the Lab. de Génie Electrique de Paris, UMR 8507 CNRS, University of Supelec, Paris 6 and 11, 91192 Gif-Sur-Yvette, France (e-mail: bouillault@lgep.supelec.fr; razek@lgep.supelec.fr).

Publisher Item Identifier S 0018-9464(02)02532-3.

J.-L. Lions

II. The Model

The mathematical model describing the eddy current problem in the conductors at low frequencies is given by the quasi-stationary Maxwell's equations. One may eliminate the electric field $\mathbf{E}$ or the current density $\mathbf{J}$ and set up a formulation in terms of the magnetic field $\mathbf{H}$ [3]. Here, we consider the alternative which consists of eliminating $\mathbf{H}$ and the magnetic induction $\mathbf{B}$ by means of a *modified magnetic vector potential* $\mathbf{A}$. In this formulation, however, we have to ensure the uniqueness of the potential in the nonconducting parts. This can be done by imposing a gauge condition [1], but we adopt an approach similar to the one presented in [7]. For a current density $\mathbf{J} = \sigma\mathbf{E} + \mathbf{J}_s$, we introduce a vector $\mathbf{T}$ such that the source current $\mathbf{J}_s = \operatorname{curl}\mathbf{T}$. Starting with a vector in the space orthogonal to $\ker(\operatorname{curl})$, the conjugate gradient algorithm applied to the final algebraic system generates, at each iteration, a solution which is again in the space orthogonal to $\ker(\operatorname{curl})$. This guarantees the potential's uniqueness; moreover, the approach is still valid in a domain decomposition framework.

Let Ω be an open set in $\mathbb{R}^3$ containing a conducting part Ω_c and a nonconducting part Ω_{nc}. We introduce the vector potential $\mathbf{A}$ such that $\mathbf{B} = \operatorname{curl}\mathbf{A}$ in Ω, $\mathbf{A} = -\int_0^t \mathbf{E}(t')\,dt'$ in Ω_c and whose tangential component $(\mathbf{A})_{\tau,\partial\Omega} = \mathbf{0}$ on $\partial\Omega$. We assume that the magnetic permeability μ and the electric conductivity σ are linear, bounded, scalar functions of the space variable $\mathbf{x}$; then the equation we solve reads

$$\sigma\frac{\partial\mathbf{A}}{\partial t} + \operatorname{curl}\left(\frac{1}{\mu}\operatorname{curl}\mathbf{A}\right) = \mathbf{J}_s. \tag{1}$$

The first step in the application of a domain decomposition method consists in dividing the considered domain into a finite number of subdomains. The initial problem (1) is then reformulated in each subdomain. Searching the solution of the problem in Ω is equivalent to looking for the solutions of the subproblems which satisfy in addition some transmission conditions at the interface between adjacent subdomains. In our case, dealing with rotating structures, we divide the domain Ω into at least two subdomains Ω_1 and Ω_2 separated by the interface Γ; Ω_1 can rotate around the z-axis with an angular speed ω. We call r_t the rotation operator at time t which rotates the domain Ω_1 by the angle $\theta = \omega t$ and r_{-t} the inverse operator. We assume the existence of a *reference* configuration, say, $\Omega(0) = \Omega_1(0)\cup\Omega_2$, and we denote by $\Omega(t) := r_t(\Omega_1(0))\cup\Omega_2$: the material particle occupies a definite position $\mathbf{x}$ in the reference domain $\Omega_1(0)$ and its changing position in the *actual* configuration $\Omega_1(t)$ at time t will be given by $r_t(\mathbf{x})$. Denoting by $\mathbf{A}_k$ the restriction of $\mathbf{A}$ to

0018–9464/02$17.00 © 2002 IEEE

Ω_k ($k = 1, 2$), in the "piecewise Lagrange approach" we look for two fields $\mathbf{A}_1$ and $\mathbf{A}_2$ satisfying the problem equation (1) in Ω_k and two time-dependent transmission conditions at Γ, i.e.,

$$
\begin{aligned}
&(E_k)\quad \sigma\frac{\partial \mathbf{A}_k}{\partial t} + \operatorname{curl}\left(\frac{1}{\mu}\operatorname{curl}\mathbf{A}_k\right) = \mathbf{J}_s \text{ in } \Omega_k, \quad k = 1, 2\\
&(TC_1)\quad \mathcal{R}_t(\mathbf{A}_1)_{\tau,\Gamma}(\mathbf{x}, t) = (\mathbf{A}_2)_{\tau,\Gamma}(\mathbf{x}, t) \text{ on } \Gamma\\
&(TC_2)\quad \mathcal{R}_t(\nu \operatorname{curl}\mathbf{A}_1)_{\tau,\Gamma}(\mathbf{x}, t) = (\nu \operatorname{curl}\mathbf{A}_2)_{\tau,\Gamma}(\mathbf{x}, t) \text{ on } \Gamma\\
&(BC)\quad (\mathbf{A}_1)_{\tau,\partial\Omega\cap\partial\Omega_k} = \mathbf{0} \text{ on } \partial\Omega\cap\partial\Omega_k, \quad k = 1, 2\\
&(IC)\quad \mathbf{A}_k(\mathbf{x}, 0) = \mathbf{0} \text{ in } \Omega_k, \quad k = 1, 2,
\end{aligned}
$$

where $\mathcal{R}_t(\mathbf{v})(\mathbf{x}, t) = r_t[\mathbf{v}(r_{-t}\mathbf{x}, t)]$ for any vector $\mathbf{v}$. The transmission conditions (TC_1) and (TC_2) describe, respectively, the continuity of $\mathbf{E}_{\tau,\Gamma}$ (and consequently of $\mathbf{B}_{n,\Gamma}$) and the continuity of $\mathbf{H}_{\tau,\Gamma}$ across the interface Γ.

To apply the edge element method, we rewrite the problem in variational form. Note that only the transmission condition (TC_1) is explicitely enforced on both the field $\mathbf{A}$ and test functions. The second condition (TC_2) is embedded in the variational formulation and can be recovered by integration by parts. For a fixed time t, we introduce the time-dependent functional space

$$
\begin{aligned}
\mathcal{U}^0(t) = \{&(\mathbf{A}_1, \mathbf{A}_2) \in H(\operatorname{curl}, \Omega_1) \times H(\operatorname{curl}, \Omega_2) \mid\\
&\mathcal{R}_t(\mathbf{A}_1)_{\tau,\Gamma}(\mathbf{x}, t) = (\mathbf{A}_2)_{\tau,\Gamma}(\mathbf{x}, t), \ \forall \mathbf{x} \in \Gamma,\\
&(\mathbf{A}_k)_{\tau,\partial\Omega_k\cap\partial\Omega} = \mathbf{0}, \ k = 1, 2\}. \qquad (2)
\end{aligned}
$$

The variational formulation of the problem reads: find $(\mathbf{A}_1, \mathbf{A}_2) \in L^\infty(0, T, \mathcal{U}^0) \cap H^1(0, T, \mathbf{L}^2(\Omega))$ such that

$$
\begin{aligned}
\sum_{k=1}^{2}\int_{\Omega_k} \sigma\frac{\partial \mathbf{A}_k}{\partial t}\cdot\mathbf{v}_k\, d\Omega + \int_{\Omega_k}\nu \operatorname{curl}\mathbf{A}_k\cdot\operatorname{curl}\mathbf{v}_k\, d\Omega\\
= \sum_{k=1}^{2}\int_{\Omega_k}\mathbf{T}_k\cdot\operatorname{curl}\mathbf{v}_k\, d\Omega \quad \forall(\mathbf{v}_1, \mathbf{v}_2) \in \mathcal{U}^0. \qquad (3)
\end{aligned}
$$

III. Discretization

We discretize (3) in each subdomain, using in space an edge element method and in time a first-order implicit Euler scheme. When looking for a discrete counterpart of the space $\mathcal{U}^0$, the equality $\mathcal{R}_t(\mathbf{A}_1)_{\tau,\Gamma} = (\mathbf{A}_2)_{\tau,\Gamma}$ on Γ becomes a too stringent condition since both fields are defined on *a priori* different and nonmatching grids. Currently a standard procedure for nonconforming domain decomposition methods, the mortar element method leads to impose the transmission condition (TC_1) in a weak form by means of a suitable space of Lagrange multipliers M_h. Once discretized, both domains Ω_k by two independently created meshes of tetrahedra $\mathcal{T}_{k,h}$ (h is the maximum size of all mesh tetrahedra), we introduce two edge element spaces $X_{k,h}$ as in [4] and $T_h := \{(\mathbf{v}_{2,h})_{\tau,\Gamma} \mid \mathbf{v}_{2,h} \in X_{2,h}\}$ the space of tangential components on Γ of functions in $X_{2,h}$. We choose M_h as a proper subset of T_h, such that $\dim(M_h) = \dim(T_h \cap H_0(\operatorname{curl}, \Gamma))$ as in [4]. The definition of M_h involving the edge element space $X_{1,h}$ gives a different but similar mortar method (in the mortar terminology, this means that we choose Ω_1 as the *master* and Ω_2 as the *slave*). The approximation space is

$$
\begin{aligned}
\mathcal{U}_h^0(t) = \Big\{ &(\mathbf{A}_{1,h}, \mathbf{A}_{2,h}) \in X_{1,h}\times X_{2,h} \,\Big|\, (\mathbf{A}_{k,h})_{\tau,\partial\Omega\cap\partial\Omega_k} = \mathbf{0},\\
&\int_\Gamma [\mathcal{R}_t(\mathbf{A}_{1,h})_{\tau,\Gamma} - (\mathbf{A}_{2,h})_{\tau,\Gamma}]\cdot\varphi_h\, d\Gamma = 0, \ \forall\varphi_h \in M_h\Big\}.
\end{aligned}
$$

For the time discretization in the interval $[0, T]$, let Δt be the time step and N an integer such that $T = N\Delta t$. Denoting by $t^n = n\Delta t$, $\mathbf{v}_h^n = \mathbf{v}_h(t^n)$ and $\mathcal{U}_h^0(n) = \mathcal{U}_h^0(t^n)$, the fully discretized problem reads: $\forall n = 1, \ldots, N$, find $(\mathbf{A}_{1,h}^n, \mathbf{A}_{2,h}^n) \in \mathcal{U}_h^0(n)$ such that $\forall(\mathbf{v}_{1,h}^n, \mathbf{v}_{2,h}^n) \in \mathcal{U}_h^0(n)$

$$
\begin{aligned}
\sum_{k=1}^{2}\int_{\Omega_k}\left[\sigma\frac{\mathbf{A}_{k,h}^n - \mathbf{A}_{k,h}^{n-1}}{\Delta t}\cdot\mathbf{v}_{k,h}^n + \frac{1}{\mu}\operatorname{curl}\mathbf{A}_{k,h}^n\cdot\operatorname{curl}\mathbf{v}_{k,h}^n\right] d\Omega\\
= \sum_{k=1}^{2}\int_{\Omega_k}\mathbf{T}_{k,h}^n\cdot\operatorname{curl}\mathbf{v}_{k,h}^n\, d\Omega. \qquad (4)
\end{aligned}
$$

To write the matrix form of the fully discretized problem at time t^n, we need to construct a basis of the approximation space $\mathcal{U}_h^0(n)$. The elements of the chosen basis are built from the edge element basis functions and, at the edges lying on Γ, they are linked through the matching condition stated in $\mathcal{U}_h^0(n)$. At the algebraic level, this involves a rectangular matrix Q^n that allows to couple at the sliding interface the information coming from Ω_1 and Ω_2 at time t^n. Let e_K denote an edge of the tetrahedron K and $\Xi_k = \{e_K | K \in \mathcal{T}_{k,h_k}\}$, $\Xi_k^0 = \{e_K | K \in \mathcal{T}_{k,h_k}, e_K \notin \partial\Omega_k\backslash\Gamma\}$. The edges lying on Γ are divided into three sets: $\xi^k = \{e \in \Xi_k \cap \Gamma\}$, $\xi_0^k = \{e \in \Xi_k^0 \cap \Gamma\}$, $\xi_{\partial\Gamma}^k = \xi^k \setminus \xi_0^k$. We denote by m_Γ^k, $m_{\partial\Gamma}^k$, $m_{\Gamma\setminus\partial\Gamma}^k$, and m^k the number of degrees of freedom associated to all edges belonging to ξ^k, $\xi_{\partial\Gamma}^k$, ξ_0^k, and Ξ_k, respectively. Let us denote by $\mathbf{w}^k$ the basis functions associated to edges of Ξ_k: these functions are the elements of the spaces $X_{k,h}(k = 1, 2)$. At time t^n, for each of the $m_\Gamma^1 + m_{\partial\Gamma}^2$ indices s, the coefficients q_r^s, $r = 1, m_{\Gamma\setminus\partial\Gamma}^2$, are determined by imposing the integral matching condition

$$
\int_\Gamma\left[\mathcal{R}_t(\mathbf{w}_s)_{\tau,\Gamma} - \sum_{e_r\in\xi_0^2} q_r^s(\mathbf{w}_r^2)_{\tau,\Gamma}\right]\cdot\varphi_k\, d\Gamma = 0, \quad \forall\varphi_k \in M_h.
$$

Each of these $m_\Gamma^1 + m_{\partial\Gamma}^2$ sets of $m_{\Gamma\setminus\partial\Gamma}^2$ equations can be put into the following form $C\mathbf{q}^s = D(\cdot, s)$ where $\varphi_k \in M_h$

$$
C(k, r) = \int_\Gamma (\mathbf{w}_r^2)_{\tau,\Gamma}\cdot\varphi_k\, d\Gamma, \quad e_r \in \xi_0^2 \qquad (5)
$$

$$
D(k, s) = \int_\Gamma (\mathbf{w}_s)_{\tau,\Gamma}\cdot\varphi_k\, d\Gamma, \quad \begin{array}{ll}\mathbf{w}_s = \mathcal{R}_t(\mathbf{w}_s^1), & e_s \in \xi^1\\ \mathbf{w}_s = -\mathbf{w}_s^2, & e_s \in \xi_{\partial\Gamma}^2.\end{array} \qquad (6)
$$

The matching condition allows us to determine the vector $\mathbf{q}^s$ for all edges $e_s \in \xi^1 \cup \xi_{\partial\Gamma}^2$ and thus the set of basis functions on the interface. For the matrix form of problem (4), it is useful to define the coupling matrix $Q^n = C^{-1}D = [Q_1^n, Q_2^n]$ of dimension $m_{\Gamma\setminus\partial\Gamma}^2 \times (m_\Gamma^1 + m_{\partial\Gamma}^2)$. Note that C is square and the fact that it is invertible follows from the theory. The construction of Q^n is a crucial point in the implementation of the method and, in the presence of movement, it has to be rebuilt at each new configuration of the free part. We explain now an easy procedure to numerically compute the involved integrals over Γ.

In 2-D, we could intersect two different discretizations of Γ since the involved geometric entities were segments [6]. In 3-D, the intersection between two triangles (that can even live on noncoplanar surfaces, as it happens with curved interfaces) becomes

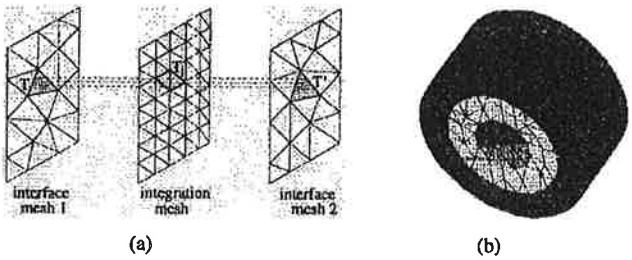

Fig. 1. (a) The integrals contained in the matching condition are computed by projecting on $(\mathcal{T}_{k,h})_{|\Gamma}$, $k = 1, 2$ the quadrature nodes defined on $\mathcal{T}^{\Gamma}_{3,h_3}$. (b) Mesh used for both domains in the *Second Example*: the cylinder basis represents the sliding interface where the matching condition has to be imposed.

a hard task. To overcome the problem we introduce, for the interface only, a new mesh $\mathcal{T}^{\Gamma}_{3,h_3}$, independent and finer (e.g., with $h_3 = h/3$) than the ones given by $(\mathcal{T}_{k,h})_{|\Gamma}$, as in Fig. 1(a) [for the case in Fig. 1(b), $\mathcal{T}^{\Gamma}_{3,h_3}$ is a triangulated disk]. The choice of introducing a new mesh is mainly due to the lack of accuracy in computing the integrals when one of the two interface meshes is used [5]. Note that $\mathcal{T}^{\Gamma}_{3,h_3}$ can be refined independently of the existing two, to improve the computational accuracy.

The computation of $\int_{\Gamma} \mathcal{R}_t(\mathbf{w}^1_s)_{\tau,\Gamma} \cdot \varphi_k \, d\Gamma$ can be done as follows: 1) we define a quadrature formula $(\omega^j_i, \mathbf{x}^j_i)$ $(j = 1, \ldots, N_q)$ on each triangle K_i of $\mathcal{T}^{\Gamma}_{3,h_3}$; 2) we build a projection operator from triangles of $\mathcal{T}^{\Gamma}_{3,h_3}$ to triangles of $(\mathcal{T}_{k,h})_{|\Gamma}$; and 3) we project each node $\mathbf{x}^j_i$ on $(\mathcal{T}_{k,h})_{|\Gamma}$ and we call $\mathbf{x}^j_{i,k}$ the projected node. Then

$$\int_{\Gamma} \mathcal{R}_t(\mathbf{w}^1_s)_{\tau,\Gamma} \cdot \varphi_k \, d\Gamma = \sum_{K_i \in \mathcal{T}^{\Gamma}_{3,h_3}} \sum_{j=1}^{N_q} \omega^j_i \, \mathcal{R}_t(\mathbf{w}^1_s)_{\tau,\Gamma}(\mathbf{x}^j_{i,1}) \cdot \varphi_k(\mathbf{x}^j_{i,2}).$$

The results we present in Section IV are obtained by using quite a fine grid $\mathcal{T}^{\Gamma}_{3,h_3}$ with $N_q = 3$. The sensibility of the numerical results to the choice of this additional mesh is under consideration.

The system we solve to get numerical results is built as follows. We start by writing, in each subdomain, the final system associated to (4) with homogeneous Neumann-type conditions on Γ. Then the two systems are coupled by means of the mortar condition.

Let $(\mathbf{A}^n_1, \mathbf{A}^n_2)$ be the solution of the fully discrete problem at time t^n: we expand it in terms of the edge element basis functions of the spaces $X_{k,h}$. We then have m^1 unknown coefficients A^1_s and m^2 unknown coefficients A^2_{τ}. We divide the unknowns in each subdomain in three blocks: the first block $\mathbf{A}^n_{k,\partial\Gamma}$ contains the unknowns associated to edges in $\xi^k_{\partial\Gamma}$, the second block $\mathbf{A}^n_{k,\Gamma\setminus\partial\Gamma}$ contains those associated to edges in $\xi^k_{\Gamma\setminus\partial\Gamma}$, and the third block $\mathbf{A}^n_{k,Int}$ to edges in $\Xi^k \setminus \xi^k$. Neither $\mathbf{A}^n_1$ nor $\mathbf{A}^n_2$ are solutions of the local problems since the two sets of values $((\mathbf{A}^n_{1,\partial\Gamma}, \mathbf{A}^n_{1,\Gamma\setminus\partial\Gamma}), \mathbf{A}^n_{2,\partial\Gamma})$ and $\mathbf{A}^n_{2,\Gamma\setminus\partial\Gamma}$ are linked one to the other by the mortar matching condition. We have

$$\mathbf{A}^n_{2,\Gamma\setminus\partial\Gamma} = [Q^n_1, Q^n_2] \left((\mathbf{A}^n_{1,\partial\Gamma}, \mathbf{A}^n_{1,\Gamma\setminus\partial\Gamma}), \mathbf{A}^n_{2,\partial\Gamma}\right)^t$$

where $Q^n = [Q^n_1, Q^n_2]$ is the rectangular full matrix of dimension $m^2_{\Gamma\setminus\partial\Gamma}$ per $m^1_{\Gamma} + m^2_{\partial\Gamma}$ obtained from the matching condition discretization at time t^n. We introduce then the following matrices:

$$\tilde{Q}^n = \begin{pmatrix} Id & 0 & 0 & 0 \\ 0 & Id & 0 & 0 \\ 0 & 0 & Id & 0 \\ Q^n_1 & 0 & Q^n_2 & 0 \\ 0 & 0 & 0 & Id \end{pmatrix}, \quad S = \begin{pmatrix} S^1 & 0 \\ 0 & S^2 \end{pmatrix}, \quad M = \begin{pmatrix} M^1 & 0 \\ 0 & M^2 \end{pmatrix}$$

with S^k, M^k denoting the local stiffness and mass matrices. Indicating by $\mathbf{y}^n$ the independent unknowns at time t^n, i.e., $\mathbf{y}^n = ((\mathbf{A}^n_{1,\partial\Gamma}, \mathbf{A}^n_{1,\Gamma\setminus\partial\Gamma}), \mathbf{A}^n_{1,Int}, \mathbf{A}^n_{2,\partial\Gamma}, \mathbf{A}^n_{2,Int})^t$, the approximated solution is computed by solving the system

$$(\tilde{Q}^n)^t \left(S + \frac{M}{\Delta t}\right) \tilde{Q}^n \mathbf{y}^n = (\tilde{Q}^n)^t \frac{M}{\Delta t} (\tilde{Q}^{n-1}) \mathbf{y}^{n-1} + (\tilde{Q}^n)^t \mathbf{f}^n.$$

To solve this system, we apply an iterative Jacobi preconditioned conjugate gradient procedure. Thanks to the mortar method philosophy, residuals can be computed in parallel. In detail, for a vector $\mathbf{v} \in \mathbb{R}^d$ with $d = m^1 + m^2 - m^2_{\Gamma\setminus\partial\Gamma}$, the matrix–vector product $(\tilde{Q}^n)^t(S + (M/\Delta t))\tilde{Q}^n\mathbf{v}$ can be done in three sequential steps: 1) we compute $\mathbf{q} = \tilde{Q}^n\mathbf{v}$ with $\mathbf{q} \in \mathbb{R}^s$ with $s = m^1 + m^2$; 2) we compute $\mathbf{p} = (S + (M/\Delta t))\mathbf{q}$ separately in each subdomain, i.e., $\mathbf{p}^k = (S^k + (M^k/\Delta t))\mathbf{q}^k$; and 3) we compute $\mathbf{w} = (\tilde{Q}^n)^t\mathbf{p}$ with $\mathbf{w} \in \mathbb{R}^d$. We have used a classical Jacobi preconditioned conjugate gradient algorithm, but the matrix–vector products are done as explained. As a consequence, there is a sensible gain in time, without involving additional memory storage. Note that the use of the third mesh $\mathcal{T}_{3,h_3}$ to compute Q^n has lead to a final system whose matrix is symmetric [5].

IV. Results and Discussion

We present some numerical results for problem (4).

First Example: We start by considering a simple stationary case where Ω is the unit cube and Γ the flat surface $\{(0.5, y, z) \mid (y, z) \in [0, 1]^2\}$. The chosen data give rise to a magnetic vector potential which is tangent to the interface. The mortar method is then used to couple nonnegligeable information. The nonconformity of the subdomain discretization at Γ is here achieved in one of two ways: either we choose the same mesh in both subdomains and we rotate one mesh 90° with respect to the other, or we consider a finer/coarser mesh in one of the subdomains. We take $\sigma = 0$ and the vector $\mathbf{T}$ such that curl $\mathbf{T} = \mathbf{J}$ is $\mathbf{T} = (0, 0, \mathrm{T}_0(x - 0.5))$ with $\mathrm{T}_0 = 10^7$ A/m. For the considered situation, the magnetic induction $\mathbf{B}$ has a maximum intensity of 3.9 Wb/m^2. In Fig. 2, we see that the information is correctly transferred from the master to the slave subdomain despite that the discretizations do not match at the interface and even when the master mesh is coarser than the slave one. Moreover, the maximum of the computed magnetic flux density, on the top of the grey scale, is equal to the analytical one.

We now investigate the precision of the method by considering the dependence of the error $(W_a - W_h)/W_a$ for the magnetic energy on the mesh parameter h. The computed value W_h for the magnetic energy is compared with the analytical one $W_a = 2.208$ MJ. In Fig. 3(a), the relative error is computed when both subdomains are discretized by the same mesh.

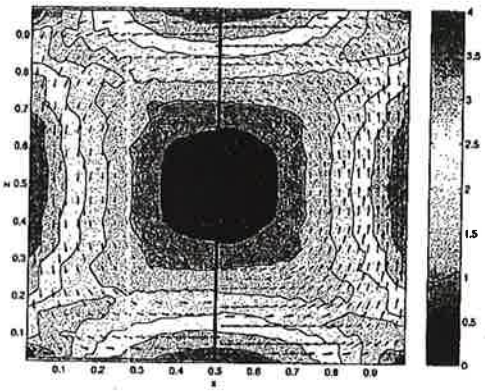

Fig. 2. Magnetic induction $\mathbf{B}$ on the section $y = 0.25$ of $[0, 1]^3$: the intensity (in Wb/m^2) and the restriction to the section of $\mathbf{B}$ computed at the tetrahedra barycenters are presented. The dark line separates the two subdomains ($h_1 = 2h_2$).

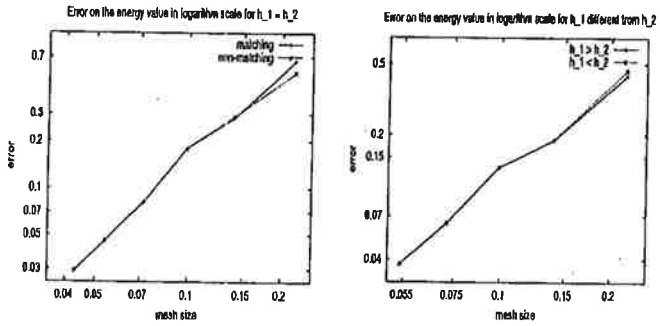

(a) (b)

Fig. 3. Relative error on the stored magnetic energy. (a) $h_1 = h_2$: the discretizations, induced on the interface by the subdomain meshes, are either conforming or nonconforming. (b) $h_1 \neq h_2$.

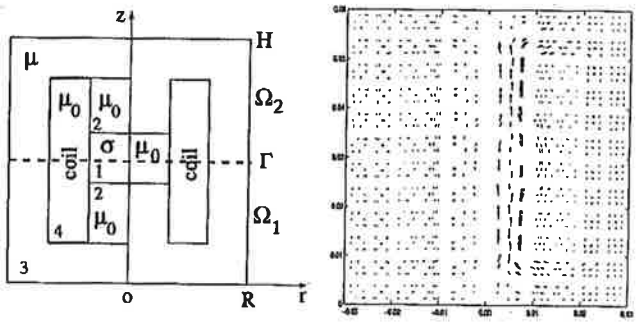

(a) (b)

Fig. 4. (a) Domain geometry on the section orthogonal to the cylinder basis: four regions with magnetic permeability $\mu_1 = \mu_2 = \mu_4 = \mu_0$, $\mu_3 = 10\mu_0$ and only $\sigma_1 \neq 0$. Region (4) is a coil of height $h = 4$ cm, internal radius $r_1 = 1$ cm, external radius $r_1 = 2$ cm, feeded with a constant density current $J = 0.125$ MA/m^2. The dashed line Γ denotes the position of the interface between the lower Ω_1 and upper Ω_2 parts. (b) Distribution of $\mathbf{B}$ when $\sigma_1 = 0$.

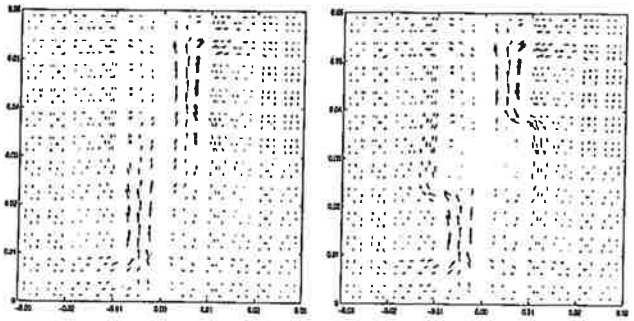

(a) (b)

Fig. 5. Distribution of $\mathbf{B}$: (left) $\sigma_1 = 0$ and Ω_1 is rotated of 180° with respect to the initial configuration (presented in Fig. 4); (right) after 20 time-iterations with $\Delta t = 5$ ms ($\sigma_1 \neq 0$) and Ω_1 rotating with $\omega = 0.5\,\pi$ rad/s.

Whether the two discretizations of Γ, induced by the subdomain meshes, match or not, the error is the same and decreases linearly with the mesh parameter h, as predicted by the theory. In Fig. 3(b), we analyze the influence of the master mesh element size h_1 on the precision of the method. The error is then computed twice, taking the master mesh finer ($h_1 = 0.5\ h_2$) or coarser ($h_1 = 2\,h_2$) than the slave one. We can observe that the error is the same in both cases and decreases linearly with h_1.

Second Example: We consider a bounded cylinder of height $H = 6$ cm and radius $R = 3$ cm with axis parallel to the z direction [see Fig. 4(a) and (b) for the mesh used in each subdomain]. We present now the distribution of $\mathbf{B} = \text{curl}\ \mathbf{A}$ in the section $\theta = 0$ orthogonal to the cylinder basis, generated by a constant density current flowing in the coils, for different values of the lower part rotating velocity ω. The coil being circular with axis parallel to the z direction and the density current $\mathbf{J}$ constant, we have that $\mathbf{T} = (\alpha r + \beta)\mathbf{e}_z$ with $\alpha = (T_1 - T_2)/(r_1 - r_2)$ and $\beta = (r_1 T_2 - r_2 T_1)/(r_1 - r_2)$ where r_i ($i = 1, 2$) are the external and internal radii of the coil and $T_1 = 0$, $T_2 = 1250$ A/m the intensity values of $\mathbf{T}$ on the boundary surfaces of radius r_i ($i = 1, 2$). Arrows indicate the restriction to the considered section of $\mathbf{B}$ computed at the tetrahedra barycenters. If $\mu_3 = \mu_0$, we have no variations of the magnetic reluctivity (the problem is invariant per rotation); in this case, if $\omega \neq 0$, there are no induced currents in region 1. As presented in Figs. 4(b) and 5(a), the stream lines of $\mathbf{B}$ follow the way of minimum magnetic reluctivity. If $\mu_3 \neq \mu_0$, the problem is no more invariant per rotation; when $\omega \neq 0$, the induced currents, flowing in region 1, expulse the field generated by the currents in the coil [see Fig. 5(a)].

REFERENCES

[1] R. Albanese and G. Rubinacci, "Solution of three dimensional eddy current problems by integral and differential methods," *IEEE Trans. Magn.*, vol. 24, pp. 98–101, 1988.

[2] <AUTHOR: PLEASE PROVIDE PAGE NUMBERS, VOLUME AND MONTH.> F. Ben Belgacem, A. Buffa, and Y. Maday, "The mortar element method for 3-D Maxwell equations: First results," SIAM J. Numer. Anal., 2001, to be published.

[3] A. Bossavit, "Edge-element computation of the force field in deformable bodies," *IEEE Trans. Magn.*, vol. 28, pp. 1263–1266, Feb. 1992.

[4] <AUTHOR: PLEASE PROVIDE PAGE NUMBERS, VOLUME AND MONTH.> F. Bouillault, A. Buffa, Y. Maday, and F. Rapetti, "The mortar edge element method in three dimensions: Applications to magnetostatics," SIAM J. Scientific Comput., 2001, to be published.

[5] <AUTHOR: PLEASE PROVIDE PAGE NUMBERS.> Y. Maday, F. Rapetti, and B. Wohlmuth, "The influence of quadrature formulas in 3-D mortar methods," in *Proc. Domain Decomposition Workshop*, Zurich, Switzerland, 2001.

[6] F. Rapetti, F. Bouillault, L. Santandrea, A. Buffa, Y. Maday, and A. Razek, "Calculation of eddy currents with edge elements on non-matching grids in moving structures," *IEEE Trans. Magn.*, vol. 36, pp. 1356–1359, Apr. 2000.

[7] Z. Ren, "Influence of the R.H.S. on the convergence behavior of the curl–curl equation," *IEEE Trans. Mag.*, vol. 32, pp. 655–658, Mar. 1996.